

Optical activation and excitation mechanisms of Er implanted in Si

S. Coffa, F. Priolo, and G. Franzò

Dipartimento di Fisica, Università di Catania, Corso Italia 57, I95129 Catania, Italy

V. Bellani*

Ecole Polytechnique Fédérale de Lausanne, Institut de Physique Appliquée, PHB-Ecublens, CH-1015 Lausanne, Switzerland

A. Carnera

Dipartimento di Fisica "Galileo Galilei," Università di Padova, Via F. Marzolo 8, I35131 Padova, Italy

C. Spinella

Istituto di Metodologie e Tecnologie per la Microelettronica, Consiglio Nazionale delle Ricerche, Corso Italia 57, I95129 Catania, Italy

(Received 16 April 1993; revised manuscript received 20 July 1993)

The several processes required to achieve Er luminescence in Si are investigated. In particular, the role of Er-O interactions to obtain the incorporation of high Er concentrations, electrically and optically active, in crystalline Si is addressed. Multiple Er and O implants were performed on *n*-type (100) Si crystals to obtain flat concentrations of $\sim 1 \times 10^{19}$ Er/cm³ and $\sim 1 \times 10^{20}$ O/cm³ over an ~ 2 - μ m-thick layer. These implants produced also a 2.3- μ m-thick amorphous Si (*a*-Si) layer. A subsequent thermal treatment at 620°C for 3 h induced the epitaxial regrowth of the whole layer and the incorporation of both Er and O in a good-quality single crystal. A further annealing at 900°C for 30 sec produced the electrical activation of the implanted Er in the presence of O, with an Er donor concentration of $\sim 8 \times 10^{18}$ /cm³ over an ~ 1.8 - μ m-thick layer. This value is more than two orders of magnitude above the maximum Er donor concentration reported in the literature, demonstrating the crucial role of O in increasing the electrically active Er concentration in crystalline Si. The optical efficiency of this sample has been studied by photoluminescence. It is seen that an enhancement by a factor of ~ 6 with respect to the literature data is obtained. Moreover, studies on the photoluminescence intensity as a function of the pump power give important information on the mechanisms underlying Er luminescence in Si and its competing phenomena. These data are presented and discussed. A plausible model based on the previous results is also presented.

I. INTRODUCTION

The expanding field of long-distance communications and local network interconnections has urged the development of new and sophisticated optoelectronic devices such as optical amplifiers, lasers, and light-emitting diodes.^{1,2} Since silicon is the semiconductor with the most mature technology, a large effort has been devoted to the realization of silicon-based optoelectronic devices. Due to the indirect band gap of Si, light emission from this material requires proper engineering such as the formation of heterojunctions. It has been demonstrated^{3,4} that the introduction of rare-earth atoms has noticeable potentiality. In fact, it is possible to have light emission from the intra-*4f* transitions of these elements. In particular the transition $I_{13/2} \rightarrow I_{15/2}$ of Er ions produces light emission at 1.54 μ m which is of particular interest in communication technology because the losses in optical fibers have a minimum at this wavelength.

The process of Er luminescence in Si is a phenomenon which involves different but equally important steps. First, Er has to be incorporated at high concentrations in Si without the formation of precipitates. Second, it has to be incorporated in its optically active 3+ state. Finally the rate of pumping of the levels involved in the transi-

tion has to be as efficient as possible.

Previous studies⁵ have demonstrated that the solubility limit of Er in Si is $\sim 10^{18}$ /cm³. At higher concentrations, in fact, precipitates are formed. Moreover the optical activity, as measured by photoluminescence, increases up to an Er concentration of $\sim 4 \times 10^{17}$ Er/cm³ and then decreases at higher concentrations.⁶ A similar trend has been observed for the electrical activation.⁷ In fact, Er has been demonstrated to present a donor behavior in Si with levels at 0.06 and 0.17 eV from the conduction band.⁷ The Er donor concentration in Czochralsky (CZ) Si increases with increasing dose up to a maximum value of 5×10^{16} donors/cm³ at concentrations of $\sim 4 \times 10^{17}$ Er/cm³. For higher Er contents the electrical activation is seen to decrease.

Electrical⁷ and optical^{6,8} activations are both increased by the presence of O. Photoluminescence and higher electrical activation are obtained in CZ Si, which contains $\sim 10^{18}$ /cm³ O atoms, while both are very limited in float zone (FZ) Si ($\sim 10^{16}$ O/cm³). These similarities suggest that electrical and optical activations are indeed correlated, i.e., the Er donor behavior might be associated with the Er³⁺ state. This state is probably the result of the formation of Er-O complexes. In fact, extended x-ray-absorption fine-structure analyses⁹ have shown that

Er is coordinated with six O atoms in CZ Si (where it is optically and electrically active) while is coordinated with Si in FZ Si (where it is optically and electrically inactive).

The pumping of Er levels is thought to occur through the recombination of $e-h$ pairs¹⁰ at the Er atoms. Therefore this pumping is strongly dependent on those processes, such as recombination at crystallographic defects or at the surface, which cause a reduction in the $e-h$ pair population. It is then important that the optically active sites are introduced in a good-quality crystal.

Recently¹¹ high concentrations of Er atoms ($\sim 10^{20}/\text{cm}^3$) have been incorporated in Si crystals by solid phase epitaxy, at $\sim 600^\circ\text{C}$, of thin ($\sim 1500 \text{ \AA}$) amorphous Si (a -Si) layers. This Er, however, though exceeding the solubility limit, seems to be inactive both electrically and optically. Erbium segregation at the moving crystal-amorphous ($c-a$) interface occurs during regrowth and has been shown to pose severe problems in obtaining the incorporation of higher Er concentrations and/or the regrowth of thicker layers.

In this paper we show that epitaxial regrowth of a 2.3- μm -thick a -Si layer doped with high concentrations of Er and O can be obtained. The presence of O is demonstrated to be critical in determining both a well-behaved regrowth of the a -Si layer and in enhancing the electrical activation of the high Er concentration ($\sim 1 \times 10^{19}/\text{cm}^3$) which is introduced in the defect-free crystal obtained from regrowth. Moreover studies on the photoluminescence behavior as a function of the laser pump power allowed us to obtain a better understanding on the processes producing luminescence and on those limiting it. These findings represent a promising step toward the feasibility of Si-based optoelectronic devices.

II. EXPERIMENT

Both CZ and FZ n -type, (100)-oriented, Si wafers were implanted by multiple Er implants at 77 K. Six different implants in the energy range 0.5–5 MeV and in the dose range 8×10^{13} – $9 \times 10^{14}/\text{cm}^2$ were used to obtain an almost constant Er concentration of $1 \times 10^{19}/\text{cm}^3$ between 0.3 and 2 μm . Some of the samples were subsequently implanted with multiple O implants in the energy range 0.15–1.4 MeV and in the dose range 1.5×10^{15} – $3.1 \times 10^{15}/\text{cm}^2$ to obtain an almost constant concentration of $10^{20}/\text{cm}^3$ in the Er-doped region. These implants produce a continuous amorphous layer extending from the surface to 2.3 μm as observed by cross sectional transmission electron microscopy (TEM).

After implantation samples were annealed in a vacuum furnace at 620°C for 3 h to induce the epitaxial regrowth of the amorphous layer and were then treated by rapid thermal annealing (RTA) at 900°C for 30 sec to activate both electrically and optically the implanted erbium.

The impurity profiles (both before and after annealing) were measured by secondary-ion mass spectroscopy (SIMS) using a CAMECA IMS-4f instrument. The Er profile was measured by using a 5.5-keV O_2^+ primary ion beam and detecting the $^{168}\text{Er}^+$ signal. In order to avoid interferences with the $^{28}\text{Si}_6^+$ signal, a high mass resolution ($\Delta M/M \approx 1/3000$) was used thus allowing

minimum detectability limits in the 10^{13} atoms/ cm^3 range when the implanted dose is low and the memory effects are therefore negligible. The oxygen profile was detected as negative ions by using a 14.5-keV Cs^+ beam. The electrically active Er concentration was measured by spreading resistance (SR) analyses. Samples for SR were beveled at an angle of 34 ft and the data were converted into carrier concentration through a code by Berkowitz and Lux.¹² Structural characterization of the samples was performed by TEM in the cross-sectional configuration using a 200-kV JEOL 2010 microscope. Samples for TEM analyses were thinned by mechanical polishing and Ar^+ -ion milling.

Photoluminescence spectra were obtained by pumping with a Kr-ion laser tuned at a wavelength of 530.9 nm. The pump power on the samples was varied in the range 0.1–1000 mW. During the measurements samples were introduced into a cryostat whose temperature could be continuously varied between 3 and 300 K. The detection apparatus consisted of a lock-in system, a 1402 Spex double spectrometer and a liquid-nitrogen-cooled Ge detector and results in an overall resolution of 15 \AA .

III. RESULTS AND DISCUSSION

In order to achieve the incorporation of a high concentration of electrically and optically active Er atoms in Si we have coimplanted Er and O to obtain almost constant profiles at a ratio 1:10. Figure 1 shows the Er and O SIMS profiles taken before and after the annealing process (620°C , 3 h) for the O-doped sample. During anneal-

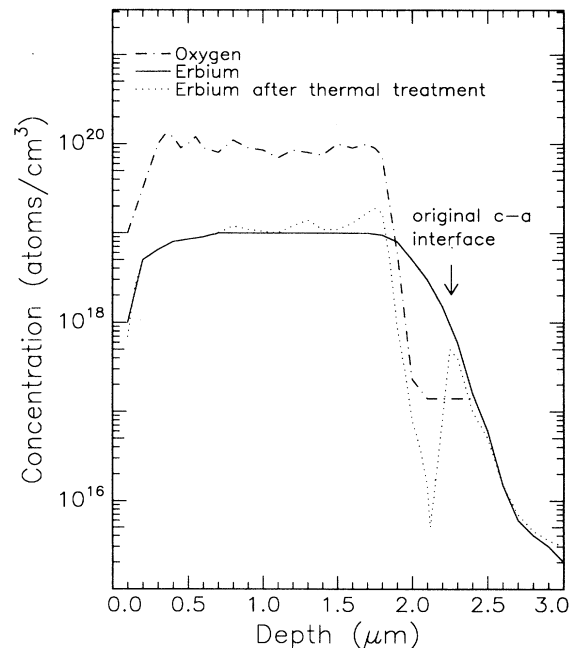


FIG. 1. Er and O profiles before and after annealing at 620°C for 3 h for multiple implants in Si. The O profiles are identical both before and after annealing. The position of the original crystal-amorphous interface is also indicated in the figure.

ing the O profile remains unmodified at a constant value of $\sim 10^{20}/\text{cm}^3$ between 0.3 and 1.8 μm . On the other hand, the Er profile changes upon annealing. A peak of Er is segregated at $\sim 2.3 \mu\text{m}$, which is where the end of range defects are probably left. Moreover, in the region between 2.3 and 1.8 μm Er has been swept by the moving *c-a* interface. As soon as Er enters the O-doped region this redistribution, however, stopped. A clear Er peak is indeed observed at 1.8 μm (which is due to the Er coming from the deeper region) and after that the Er profile is almost unchanged. This redistribution is attributed to segregation processes occurring at the moving *c-a* interface.^{11,13} While the interface is passing through, Er is partially swept into the amorphous phase and partially incorporated into the crystal, with an Er peak growing at the moving interface. This process depends on both interface velocity and Er diffusivity. Oxygen is known to retard the *c-a* interface velocity¹⁴ and to reduce Er diffusivity through the formation of Er-O complexes.¹⁵ Therefore the segregation process abruptly changes when the *c-a* interface enters the O-doped region and Er remains trapped in the regrowing crystal.

In Fig. 2 cross-sectional TEM images of both as-implanted and annealed samples are shown. Figure 2(a) shows the as-implanted sample in which a 2.3- μm -thick continuous *a*-Si layer is clearly present. After annealing this layer is transformed into a good-quality single crystal in the case of the O implanted sample [Fig. 2(b)]. A band of dislocation loops is present at the end of range (corresponding to the Er peak in SIMS) and for the rest a good crystal with a few threading dislocations traversing the whole film is observed. It is noticeable that a huge amount of Er has been incorporated in such a deep layer. Epitaxial regrowth occurred in spite of the presence of oxygen. As a matter of fact oxygen played a crucial positive role in stabilizing the Er thus allowing crystallization. This is clear from Fig. 2(c) where the annealed layer in absence of oxygen is shown. Epitaxial regrowth occurred for only $\sim 800 \text{ nm}$ and then the interface broke up with the formation of a heavily twinned material. This suggests that the Er redistribution (occurring in absence of O) makes the *c-a* interface unstable and twin formation soon occurs.

In order to establish if these effects are also correlated with the interface velocity (which is certainly smaller in presence of O) we have annealed some of the samples at lower temperatures (530 °C). The effects are indeed similar. Er segregation occurs in absence of oxygen, also with comparable interface velocities. In this case, however, interface instabilities are not observed and the whole layer can be recrystallized. The crystalline quality is poor and a very high density of dislocations, decorated by Er precipitates, is present on this sample in a 1- μm -thick surface layer [Fig. 2(c)]. Therefore Er-O interaction plays a key role on both Er incorporation and crystalline quality.

After regrowth the samples were annealed at 900 °C for 30 sec in order to activate electrically and optically the Er atoms. Once more Er-O interaction proves to be crucial in determining the electrically active fraction. In fact, in absence of O, the resistivity of the regrown layers is quite high. This is attributed to the presence of twins

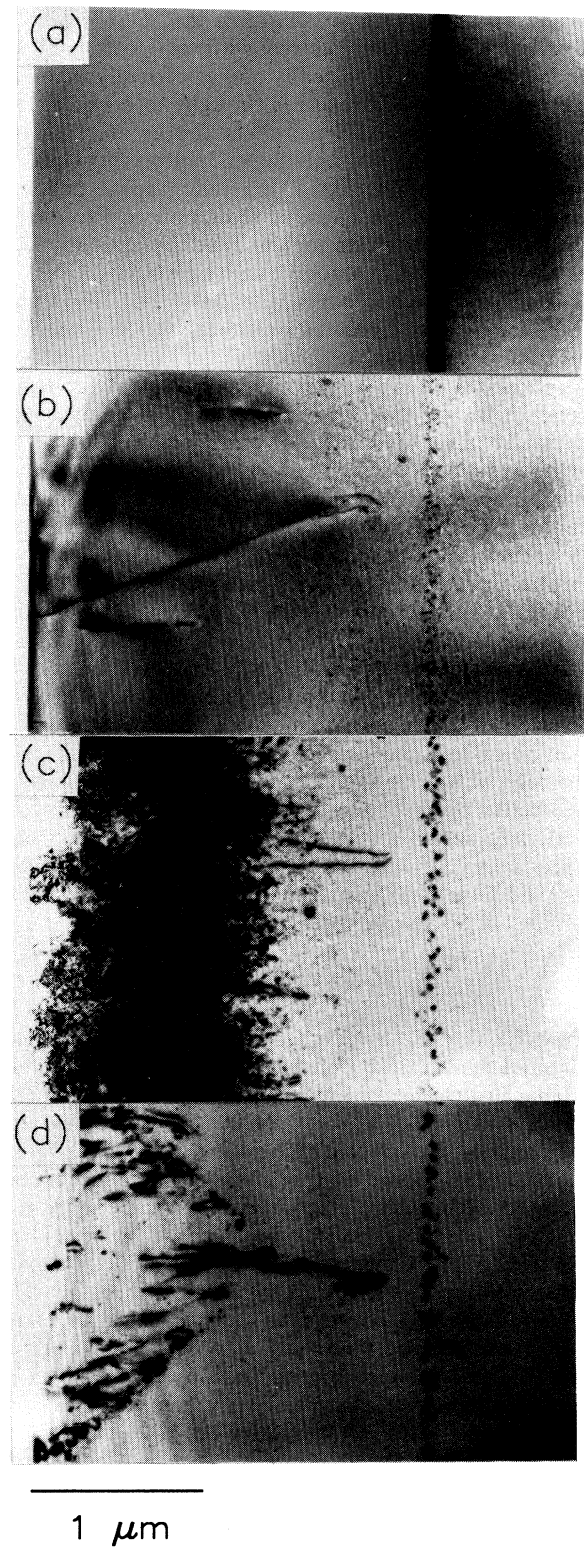


FIG. 2. Cross-sectional TEM images of the as-implanted sample (a), after annealing at 620 °C (b), (c), and at 530 °C (d). Image (b) refers to an Er + O-doped sample while (c) and (d) refer to a CZ Si sample only implanted with Er.

and/or dislocations. Moreover, a strong Er precipitation is observed after the high-temperature treatment (TEM not shown) demonstrating that the Er activation is poor. A different picture emerges in the O-implanted sample. The profile of the electrically active Er in this sample is reported in Fig. 3 (note that the chemical profile remained unchanged upon the high-temperature annealing). A donor concentration of $\sim 8 \times 10^{18}/\text{cm}^3$ flat between 0.3 and $1.8 \mu\text{m}$ is present, demonstrating that most of the Er is electrically active. The active concentration is more than 2 orders of magnitude above the maximum Er donor concentration reported in the literature ($5 \times 10^{16}/\text{cm}^3$) (Ref. 7) and is incorporated in a good-quality crystal.

If electrical and optical activations are indeed correlated it is expected that the concentration of optically active Er atoms must be quite high. We have therefore performed photoluminescence measurements at 3 K. For the sake of comparison these measurements were also performed on a reference sample. This sample was produced by Er implantation at 5 MeV to a fluence of $4 \times 10^{13}/\text{cm}^2$. It contains about the maximum amount of Er that can be introduced before the onset of precipitation and/or the formation of a continuous amorphous layer. Therefore it represents one of the best samples which can be produced by the procedures so far reported in the literature.⁶

The photoluminescence (PL) spectra for these two samples are reported in Fig. 4. For these spectra a pump power of 120 mW was used. The intensity is more than a factor of 2 higher for the epitaxially regrown O-doped sample than for the reference sample. However, the es-

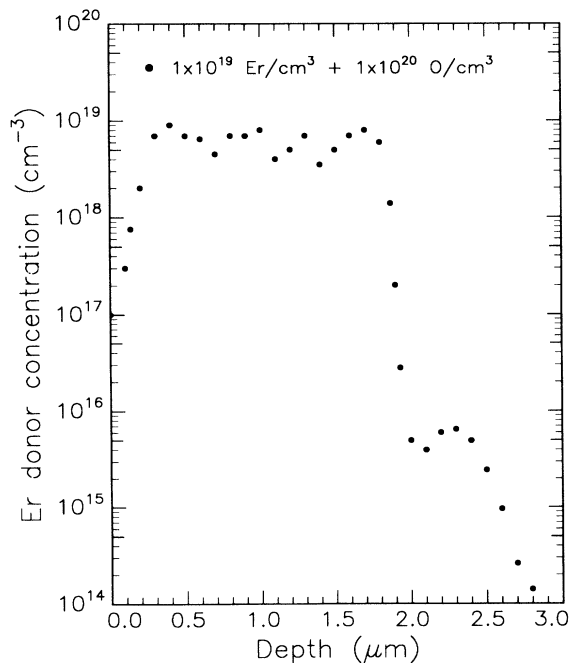


FIG. 3. Er donor concentration as measured by SR for a sample doped with constant concentrations of $1 \times 10^{19} \text{ Er}/\text{cm}^3$ and $1 \times 10^{20} \text{ O}/\text{cm}^3$, regrown at 620°C for 3 h and further annealed at 900°C for 30 sec.

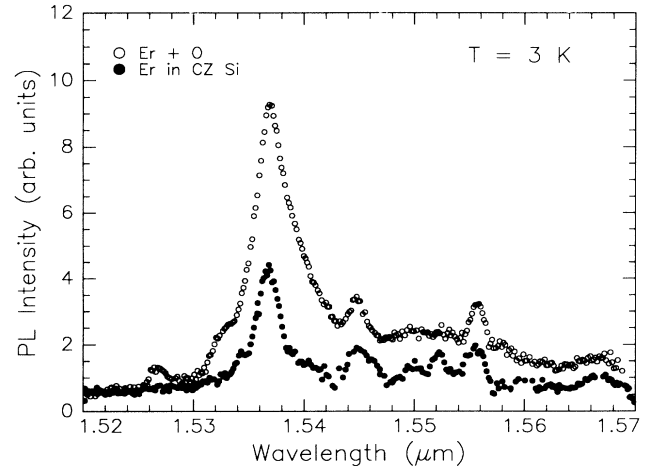


FIG. 4. Photoluminescence intensity spectra at 3 K for the Er + O-doped sample ($1 \times 10^{19} \text{ Er}/\text{cm}^3 + 1 \times 10^{20} \text{ O}/\text{cm}^3 + 620^\circ\text{C}$ 3 h + 900°C 30 sec) and an Er in CZ Si reference sample ($4 \times 10^{13} \text{ Er}/\text{cm}^2$ in CZ Si + 900°C 30 sec). The pumping wavelength was 530.9 nm and the pump power was 120 mW.

timination of the ratio between the number of optically active sites in the two samples is not an easy task. Photoluminescence intensity, in fact, depends not only on the total number of optically active sites but also on the pumping efficiency for these sites and on the balance between radiative and nonradiative decay of the excited atoms. These two last steps are critically dependent on the crystal quality. In particular the pumping is thought to occur through the recombination of $e-h$ pairs at the Er atoms or through other electron- and hole-mediated processes. It is therefore affected by those processes, such as recombination at defects and/or at the surface, which reduce the concentration of $e-h$ pairs. A hint on which process really limits the pumping efficiency may be obtained by measuring the photoluminescence intensity as a function of pump power at different temperatures. The results obtained for the two samples are reported in Fig. 5 at 3 K (a), 70 K (b), and 140 K (c). Note that the vertical scale is different in the three cases. For the reference sample (Er in CZ, circles) the photoluminescence intensity increases with pump power and eventually saturates. However, both the saturation level and the pump power at which saturation occurs strongly depend on temperature. The saturation level decreases by a factor of 2.5 on going from 3 to 70 K and by a further factor of 2.3 on going from 70 to 140 K. The existence of a saturation suggests that all the Er atoms might be excited. Therefore the factor limiting the luminescence yield is not the excitation due to the lack of $e-h$ pairs but the Er content. The difference in the saturation level at different temperatures is possibly due to a difference in the radiative lifetime of the excited Er atoms. Alternatively this difference should be attributed to a temperature dependence of the maximum fraction of Er atoms that can be excited. A possible reason for this temperature depen-

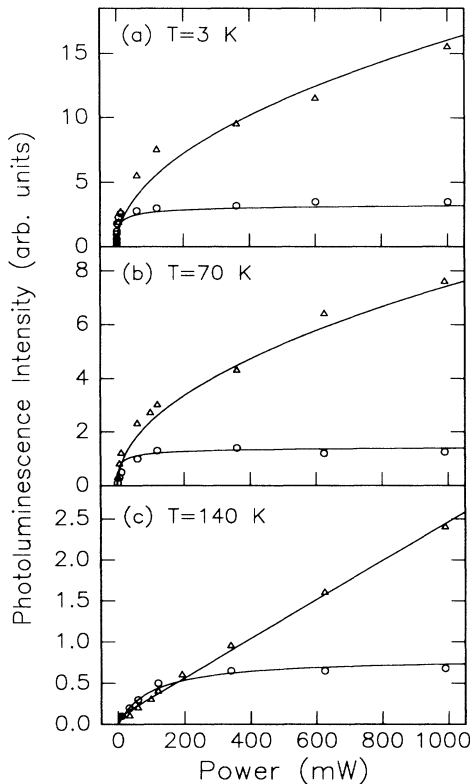


FIG. 5. Photoluminescence intensity as a function of the pump power for both an Er + O-doped sample (triangles) and Er in CZ Si reference samples (circles). Data at 3 K (a), 70 K (b), and 140 K (c) are shown. Note that the y scales are different in the three cases. The continuous lines are drawn to guide the eye.

dence could be associated with the donor behavior of active Er atoms. In fact, if as a speculation, we assume that pumping can occur only at neutral donors, the ionization of Er donors with increasing temperature will play a role in decreasing the sites that can be pumped. At the moment it is not possible to discriminate between these two possibilities.

The temperature dependence of the pump power at which saturation occurs indicates, instead, that the pumping efficiency of the Er atoms reduces with increasing temperature. This is due both to a reduced lifetime of the excited state through alternative nonradiative paths and to the fact that the number of $e-h$ recombination events, not ending with the excitation of an Er atom, increases with temperature. Recombination of $e-h$ pairs in Si can occur through Auger mechanisms, both interband and impurity mediated, through exciton recombination, via deep traps or at surface states.¹⁶ While Auger mechanisms are almost temperature independent, the efficiency of deep traps and surface states strongly increase with temperature thus reducing the $e-h$ pairs population. Therefore in order to obtain the same number of excitation events higher and higher powers are required as the temperature increases.

When measuring photoluminescence intensity as a

function of temperature at a fixed pump power two different contributions are then simultaneously present. First of all, the effect of the lifetime of the excited level. Second, the fact that, if the pump power is not sufficient to reach saturation at all the temperatures, a different number of excited Er atoms are present in the different cases. This is clear when comparing the intensity ratios at 3 and 140 K at two different pump powers on the reference sample: at 10 mW this ratio is 35 while at 300 mW it is ~ 6 . In order to separate these two contributions measurements of the luminescence intensity as a function of the pump power have to be performed at the different temperatures.

In Fig. 5 the data of the O-doped sample are also reported (Er + O, triangles). At all temperatures the luminescence intensity increases with the pump power but saturation is not achieved in the explored power range. This indicates that in all cases only a fraction of the Er atoms is excited and the limiting step for higher luminescence is then the efficient pumping of the optically active sites. While a strong effort has been devoted in achieving the incorporation of high concentrations of optically active sites in Si, the major role of pumping efficiency in determining the luminescence yield has been probably not completely recognized. Several features of the curves in Fig. 5 are noteworthy. The intensity increases less than linearly at low temperatures (3 and 70 K) while a linear increase is observed at 140 K. The sub-linear dependence at low temperatures is present also in the reference sample in the region well before saturation (this feature is not evident from Fig. 5 due to the x scale). Therefore sublinear and linear behaviors are not peculiar of the O-doped sample and might be determined by the different mechanisms which control the $e-h$ pair population at the different temperatures. Moreover at low pump powers (before saturation in the reference sample) the luminescence intensity is quite similar for the two samples. Large differences are instead observed at high pump powers, as the reference intensity saturates while that of the O-doped sample continuously increases. In fact, at 3 K the intensity ratio between the O-doped sample and the reference sample is 1 at 10 mW, ~ 4 at 600 mW, and ~ 6 at 1000 mW. Therefore comparing the luminescence of different samples at a fixed pump power is not always fair. This will certainly give important information on the ratios between the optically active sites in the two samples only if the pump power is high enough that both of the samples are at the saturation level. In all other cases the ratio critically depends on power.

IV. MECHANISMS

On the basis of the experimental results so far reported the following plausible scenario can be proposed for Er luminescence in Si.

Recent calculations¹⁰ have shown that the excitation mechanism of rare-earth atoms in semiconductors occurs most likely through a resonant Auger process in which an $e-h$ pair recombines and, as a result, the excitation of a $4f$ shell electron in the rare-earth atom is achieved.

We propose that for Er in Si this process occurs

through the recombination of an exciton bound to the rare-earth atom. This is still an Auger-type process where the exciton population plays a major role. This picture seems to be plausible since exciton recombination in Si is known to be a very efficient process.¹⁷⁻¹⁹ Therefore, under this assumption, the luminescence is controlled by the steady-state population of excitons. First of all let us calculate the steady-state exciton concentration.

The density of excitons is given by the following rate equation:²⁰

$$\frac{dn_{\text{ex}}}{dt} = anp - \frac{n_{\text{ex}}}{\tau_{\text{ex}}} - bn_{\text{ex}}n - bn_{\text{ex}}p, \quad (1)$$

where n_{ex} is the exciton concentration, n and p are the electron and hole concentrations, respectively, τ_{ex} is a recombination lifetime, and a and b are rate coefficients. The first term in Eq. (1) is the rate of formation of excitons, the second term is the annihilation rate, while the last two terms represent the rate of annihilation stimulated by electrons or holes, i.e., an Auger-type decay ending up with the exciton recombination and with the ejection of a fast electron (or hole).

The rate equation giving the carrier concentration instead is

$$\frac{dn}{dt} = G_l - \frac{n}{\tau_{\text{tr}}} - an^2 - cn^3 \quad (2)$$

being G_l the pump generation rate, τ_{tr} the lifetime due to the recombination at deep traps, an^2 the recombination rate through exciton formation, and cn^3 the recombination through an Auger process. The most effective type of recombination depends on both temperature and sample preparation. At low temperatures and in good-quality crystals, assuming that recombination through excitons prevails, the steady-state carrier concentration is

$$n = \left[\frac{G_l}{a} \right]^{1/2}. \quad (3)$$

At high temperatures when recombination at deep traps is by far the most efficient process, the steady-state carrier concentration will instead be

$$n = G_l \tau_{\text{tr}}. \quad (4)$$

The steady-state exciton concentration $n_{\text{ex}}^{\text{eq}}$ can be obtained by solving Eq. (2) to obtain the equilibrium carrier concentration and substituting this value in Eq. (1). The value of $n_{\text{ex}}^{\text{eq}}$ is therefore dependent on the pump generation rate and on both the mechanisms controlling free carrier recombination and on those controlling exciton recombination. The overall process is therefore critically dependent on temperature and crystal quality.¹⁹

Free excitons may be captured by an Er atom to form a bound exciton system. Indeed the formation of bound excitons at donors is a well-known process.¹⁶ Once there the exciton recombination can occur through several different routes. One of these can end up into the excitation of a 4*f*-shell Er electron.

Under this assumption the rate equation for Er excitation is given by

$$\frac{dN_{\text{Er}}^*}{dt} = \frac{n_{\text{ex}}^b}{\tau^*} \left[1 - \frac{N_{\text{Er}}^*}{N_{\text{Er}}} \right] - \frac{N_{\text{Er}}^*}{\tau_d} \quad (5)$$

being N_{Er}^* the concentration of excited Er atoms, n_{ex}^b the bound exciton concentration, τ^* a characteristic time for the Er excitation process, N_{Er} the total optically active Er concentration, and τ_d the deexcitation time of the excited Er atoms by either radiative or nonradiative mechanisms. The first term in Eq. (5) is the rate of excitation events. This rate is limited by the number of excitons when the exciton concentration is well below the Er concentration. This is due to the fact that the trapping cross section of a free exciton to a donor is quite large¹⁷ and therefore most of the excitons in the Er-doped region become trapped to an Er atom. However, this rate is limited by the Er concentration as soon as the number of excitons increases and most of the Er atoms are excited; this is taken into account by the normalizing factor $(1 - N_{\text{Er}}^*/N_{\text{Er}})$. The second term in Eq. (5) takes instead into account the deexcitation processes. At the steady state the concentration of excited Er atoms will be

$$N_{\text{Er}}^* = \frac{n_{\text{ex}}^b}{\frac{n_{\text{ex}}^b}{N_{\text{Er}}} + \frac{\tau^*}{\tau_d}}. \quad (6)$$

The luminescence intensity is therefore given by

$$I \propto \frac{N_{\text{Er}}^*}{\tau_{\text{rad}}} = \frac{1}{\tau_{\text{rad}}} \frac{n_{\text{ex}}^b}{\frac{n_{\text{ex}}^b}{N_{\text{Er}}} + \frac{\tau^*}{\tau_d}}, \quad (7)$$

where τ_{rad} is the lifetime of the radiative decay.

The present description can qualitatively explain all the features of the experimental data reported in Fig. 5. In fact, when $n_{\text{ex}}^b/N_{\text{Er}} \gg \tau^*/\tau_d$ then, from Eq. (6), $N_{\text{Er}}^* \simeq N_{\text{Er}}$, i.e., the process is limited by the amount of Er atoms. Under these conditions, which are achieved at high pump powers, the luminescence intensity saturates. This is in agreement with the results shown for the reference sample in Fig. 5. In fact, being the number of optically active sites in this sample quite low, saturation can be achieved in the power range we have explored. On the other hand, if $n_{\text{ex}}^b/N_{\text{Er}} \ll \tau^*/\tau_d$ then $N_{\text{Er}}^* \simeq n_{\text{ex}}^b \tau_d / \tau^*$ [from Eq. (6)], i.e., the number of excitons is the limiting factor for the Er excitation and the photoluminescence intensity increases with pump power. This regime is operative at low pump powers and/or when the optically active Er concentration is very high. This behavior is therefore thought to occur in the case of the reference sample at low powers and in the case of the O-doped sample at all the pump powers explored in the present paper. The mechanism we have proposed appears therefore to be plausible although we cannot exclude that different mechanisms are contemporarily operative and become dominant under different conditions.

A detailed and quantitative description of the data would require a complete comprehension of the phenomena controlling the bound exciton concentration, such as

free carrier and exciton recombination. A direct comparison between Eq. (7) and the experimental results, which would be possible only under several critical assumptions for the estimation of the many parameters present in Eqs. (1) and (2) was therefore not attempted.

V. CONCLUSIONS

In conclusion, we have shown that high concentrations of electrically active Er atoms in Si can be achieved through the solid phase epitaxial growth of Er and O coimplanted amorphous Si layers. The presence of high O concentrations promotes the electrical activation of an Er concentration of $\sim 8 \times 10^{18}/\text{cm}^3$, i.e., more than two orders of magnitude above literature data. Photoluminescence of these samples has been measured and compared with that of a standard reference sample. In particular photoluminescence measurements as a function of the pump power gave important information on

the mechanisms producing luminescence and on those limiting it. It has been shown that luminescence can be limited by either the number of optically active sites or by the pumping efficiency. On the basis of these results we have proposed a possible mechanism for Er luminescence in Si. The pumping of the active sites might occur through the recombination of an exciton bound to an Er donor ending up with the excitation of a 4f-shell electron.

ACKNOWLEDGMENTS

We wish to thank J. L. Staehli of the Ecole Polytechnique Fédérale de Lausanne (Switzerland) for the use of his photoluminescence apparatus. We are sincerely indebted to S. Pannitteri for the expert preparation of the samples for TEM analyses. Thanks are also due to A. Giuffrida and A. Marino for technical assistance. This work has been supported in part by GNSM-CNR.

*Permanent address: Dipartimento di Fisica "A. Volta," Università di Pavia, Via Bassi 6, I27100 Pavia, Italy.

¹A. M. Glass, *Science* **235**, 1003 (1987).

²Y. H. Xie, E. A. Fitzgerald, and Y. J. Mii, *J. Appl. Phys.* **70**, 3223 (1991).

³H. Ennen, J. Schneider, G. Pomrenke, and A. Axmann, *Appl. Phys. Lett.* **43**, 943 (1983).

⁴H. Ennen, G. Pomrenke, A. Axmann, W. Haydl, and J. Schneider, *Appl. Phys. Lett.* **46**, 381 (1985).

⁵D. J. Eaglesham, J. Michel, E. A. Fitzgerald, D. C. Jacobson, J. M. Poate, J. L. Benton, A. Polman, Y. H. Xie, and L. C. Kimerling, *Appl. Phys. Lett.* **48**, 2797 (1991).

⁶J. Michel, J. L. Benton, R. I. Ferrante, D. C. Jacobson, D. J. Eaglesham, E. A. Fitzgerald, Y. H. Xie, J. M. Poate, and L. C. Kimerling, *J. Appl. Phys.* **70**, 2672 (1991).

⁷J. L. Benton, J. Michel, L. C. Kimerling, D. C. Jacobson, Y. H. Xie, D. C. Eaglesham, E. A. Fitzgerald, and J. M. Poate, *J. Appl. Phys.* **70**, 2667 (1991).

⁸P. N. Favennec, H. L'Haridon, D. Moutonnet, M. Salvi, and M. Gauneau, *Jpn. J. Appl. Phys.* **29**, L521 (1990).

⁹D. C. Adler, D. C. Jacobson, D. J. Eaglesham, M. A. Marcus, J. L. Benton, J. M. Poate, and P. H. Citrin, *Appl. Phys. Lett.*

61, 2181 (1992).

¹⁰S. Schmitt-Rink, C. M. Varna, and A. F. J. Levi, *Phys. Rev. Lett.* **66**, 2782 (1991).

¹¹A. Polman, J. S. Custer, E. Snoeks, and G. N. Van Den Hoven, *Appl. Phys. Lett.* **62**, 507 (1993).

¹²H. L. Berkowitz and R. A. Lux, *J. Electrochem. Soc.* **18**, 1137 (1981).

¹³J. M. Poate, J. Linnros, F. Priolo, D. C. Jacobson, J. L. Batstone, and M. O. Thompson, *Phys. Rev. Lett.* **60**, 1322 (1988).

¹⁴E. F. Kennedy, L. Csepregi, J. W. Mayer, and T. W. Sigmund, *J. Appl. Phys.* **48**, 4241 (1977).

¹⁵F. Priolo, S. Coffa, G. Franzò, C. Spinella, A. Carnera, and V. Bellani, *J. Appl. Phys.* (to be published).

¹⁶For a review, see, for example, *Solid State Electron.* **21**, Nos. 11/12 (1978).

¹⁷W. Schmid, *Solid State Electron.* **21**, 1285 (1978); W. Schmid, *Phys. Status Solidi B* **84**, 529 (1977).

¹⁸P. T. Landsberg, *Phys. Status Solidi* **41**, 457 (1970).

¹⁹G. Davies, *Phys. Rep.* **176**, 83 (1989).

²⁰P. T. Landsberg, in *Handbook on Semiconductors*, edited by T. S. Moss (North-Holland, Amsterdam, 1982), Vol. 1, p. 359.

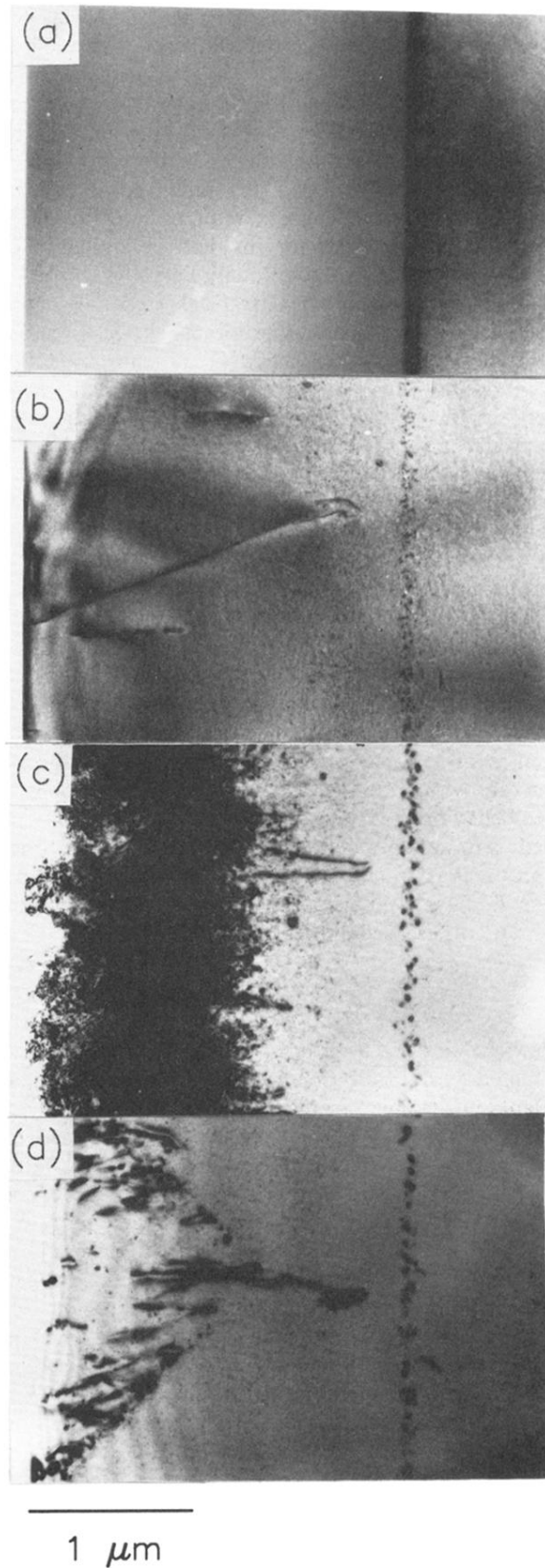


FIG. 2. Cross-sectional TEM images of the as-implanted sample (a), after annealing at 620°C (b), (c), and at 530°C (d). Image (b) refers to an Er + O-doped sample while (c) and (d) refer to a CZ Si sample only implanted with Er.